

Ion-Molecule Reactions of Vibrationally State-Selected NO^+ with Small Alkyl Halides

Thomas Wyttenbach and Michael T. Bowers*

Department of Chemistry, University of California, Santa Barbara, California 93106 (Received: May 21, 1992; In Final Form: July 23, 1992)

The effects of vibrational excitation in $\text{NO}^+(v = 0-5)$ on its reactivity with small alkyl halides ($\text{C}_n\text{H}_{2n+1}\text{X}$; $n = 1-3$; $\text{X} = \text{Cl}, \text{Br}, \text{I}$) have been investigated under thermal translational conditions. The method combines resonance enhanced multiphoton ionization to form state-selected $\text{NO}^+(v)$ and Fourier transform ion cyclotron resonance techniques to trap, react, and detect ions. Besides vibrational quenching of $\text{NO}^+(v > 0)$, which is found to be very efficient with alkyl halides, three reaction channels are observed: charge transfer, halide transfer, and $\text{C}_n\text{H}_{2n}\text{NO}^+$ formation. Branching ratios and rate constants have been determined for the different channels as a function of the $\text{NO}^+(v)$ vibrational energy. Endoergic charge transfer is efficiently driven by vibrational excitation. Halide transfer is the major channel if it is significantly exothermic for $\text{NO}^+(v = 0)$. If this is not the case, adding vibrational energy in $\text{NO}^+(v)$ is only marginally effective in driving this channel. The data suggest that rearrangements in NO^+ -alkyl halide reaction intermediates and in carbonium ions are very rapid. The $\text{C}_n\text{H}_{2n}\text{NO}^+$ formation channel is only observed with *n*-propyl and isopropyl chloride where it is dominant for $\text{NO}^+(v = 0)$. Increasing vibrational excitation inhibits $\text{C}_3\text{H}_6\text{NO}^+$ formation. The results are discussed in terms of possible reaction mechanisms.

Introduction

Reactions of vibrationally state-selected molecular ions with neutral molecules is a relatively new, interesting, and unexplored area of chemical dynamics. Only a relatively small number of studies have been reported,¹ and in most cases the reactant ions are at translational energies far above thermal. Perhaps the most widely used technique employs coincidence methods² which really select reactant ion energy and not vibrational state. In principle, these studies can be carried out near thermal translation energies, but extremely low signal levels make both the experiments and their interpretation difficult. The monitor ion method³ has been used to study reactant ions with relatively narrow distributions of vibrational states, and since these studies are conducted in flow tubes, the reactants are translationally thermal.

A novel method has been developed that uses charge-transfer reactions to form vibrationally excited product ions in the source of a tandem ICR instrument.⁴ By measuring the translational energy of the products and by carefully selecting the charge-transfer reagents, a fairly narrow range of product vibrational states is formed. These specially prepared ions are then injected into the reaction cell of the tandem ICR. This method has the advantages that a very broad range of internal energies can be generated, and the reactions take place at near thermal energies.

Finally, resonance enhanced multiphoton ionization (REMPI) has been utilized to form state-selected reactant ions.^{1b,5} The ability to unambiguously vary the reactant ion over a broad range of vibrational states is a big plus for this method. Applications to date have only been possible for translationally hot ions^{6a} or suprathreshold ions.^{1b,6b} As will be discussed shortly, we have taken the REMPI method and coupled it to an FT-ICR spectrometer, allowing both vibrational state selection and translationally thermal reactant ions. In this paper we will apply the method to reactions of $\text{NO}^+(v)$ with small alkyl halides.

The chemistry of vibrationally state-selected $\text{NO}^+(v)$ reacting with alkyl halides is particularly interesting because some reaction paths are endothermic for low vibrational excitation of NO^+ but exothermic for higher vibrational states over the range of states available to us: $0 \leq v \leq 5$. Among these reactions are charge transfer and halide ion transfer. The questions are whether or not a reaction "turns on" as soon as it is energetically possible and how it competes with other accessible channels. For example, charge-transfer reactions of NO^+ have been observed with methyl and ethyl halides⁷⁻¹³ and halide ion transfers with larger organic halides,¹⁴ but competition between the two pathways as vibrational energy changes has not been addressed.

Charge-transfer processes with small alkyl bromides and iodides have extensively been employed to "monitor" vibrationally excited NO^+ .⁷⁻¹³ To monitor an excited ion in this context means to take

advantage of the fact that the excited ion reacts with a certain monitor molecule, whereas the same ion in a less excited state does not react. In this fashion, CH_3I was used to monitor $\text{NO}^+(v > 0)$ by a charge-transfer process. In most cases^{7-10,12} the following reasonable, but experimentally not proven, assumption had to be made: exoergic charge-transfer reactions $\text{NO}^+(v > 0) + \text{CH}_3\text{I}$ are fast, but the corresponding reaction of $\text{NO}^+(v = 0)$, which is endoergic, does not proceed. The CH_3I monitor technique was employed in both selected ion flow drift tube (SIFDT)^{7,8,10} and ion cyclotron resonance (ICR)^{9,11-13} instruments to determine the ratio of $[\text{NO}^+(v > 0)]:[\text{NO}^+(v = 0)]$ in a variety of circumstances. These include electron impact ionization of NO^+ ,⁷⁻¹⁰ vibrational relaxation of $\text{NO}^+(v > 0)$ in collisions with different neutral molecules;^{7,8,10} and measurement of the radiative lifetime of $\text{NO}^+(v = 1)$.^{9,11-13} The same method was used to monitor $\text{NO}^+(v = 1)$ with $\text{C}_2\text{H}_5\text{I}$,^{12,13} $\text{NO}^+(v = 4)$ with $\text{C}_2\text{H}_5\text{Br}$ ¹³ and $\text{NO}^+(v = 5)$ with CH_3Br ¹³ in order to study radiative vibrational relaxation of $\text{NO}^+(v)$.

In most of the work mentioned above,^{7-10,12} $\text{NO}^+(v)$ was formed by electron impact ionization, which leads to an unknown distribution of vibrational ionic states. Therefore, data analysis had to be based on the assumption that exoergic charge-transfer reactions proceed rapidly and that this rate (for exoergic reactions) is independent of the vibrational state of $\text{NO}^+(v)$. Thus, $\text{NO}^+(v)$ ions were divided into two groups: those with enough vibrational excitation to react with the monitor molecule and those with too little vibrational energy to react. Ions within a group were assumed to be detected equally efficiently by the monitor reaction. In order to get some experimental evidence for the correctness of this hypothesis, Morris et al. studied the reactivity of NO^+ with CH_3I .¹⁰ $\text{NO}^+(v)$ was formed by electron impact ionization in a SIFDT instrument. The analysis of the NO^+ signal as a function of the CH_3I inlet flow rate yielded a bimodal NO^+ decay, suggesting two rates of NO^+ loss. According to the assumption above, the quicker component ($1.9 \times 10^{-9} \text{ cm}^3 \text{ s}^{-1}$) was assigned to $\text{NO}^+(v > 0)$ charge transfer and the slow component ($\sim 10^{-10} \text{ cm}^3 \text{ s}^{-1}$) to general ion loss processes, including clustering.

In contrast to the results of Morris et al. and to the basic assumptions of the monitor ion method, studies on the $\text{NO}^+/\text{CH}_3\text{I}$ system employing resonance enhanced multiphoton ionization (REMPI) to form state-selected $\text{NO}^+(v)$ ^{11,13} indicated that exothermicity alone is not sufficient to determine the reactivity of a charge-transfer reaction. For example, $\text{NO}^+(v = 1)$ seemed to react surprisingly slowly with CH_3I , but $\text{NO}^+(v = 2)$ reacted fast, as expected. One of the goals of this work is to investigate this matter.

While methyl and ethyl halides either undergo charge-transfer reactions or are nonreactive with $\text{NO}^+(v)$, the chemistry of larger

organic halides reacting with NO⁺ is much more complex. A common reaction path, observed for (CH₃)₃CCl, (CH₃)₂CHCl, and C₆H₅CH₂F,¹⁴ is halide ion transfer yielding neutral XNO (X = F, Cl). Other paths are HX and HXNO⁺ formation when the facile anion transfer reaction is endothermic and when the alkyl halide possesses a β-hydrogen.¹⁴ In the present study C_nH_{2n+1}X (n = 1–3; X = Cl, Br, I) will be investigated using vibrationally state-selected NO⁺(*v*) for *v* = 0–5, and competition between the various reaction pathways explored.

Experimental Section

Experiments were performed on a Fourier transform ion cyclotron resonance (FT-ICR) instrument which has been described in detail elsewhere.^{15b} State-selected NO⁺(*v*) ions were produced by REMPI under conditions similar to those previously described.¹³ Only a very brief summary of the experimental events during one data cycle will follow.

A pulsed valve is opened for ~100 μs to form a pulse of NO gas which is skimmed and enters the differentially pumped vacuum chamber containing the ICR cell. The NO pulse is intersected with a pulsed laser beam in the center of the ICR cell (excimer pumped dye laser, frequency-doubled for λ < 330 nm, 3–6 mJ per pulse, focused by a 5-cm focal length lens). A 2+1 REMPI through the C²Π,*v* state of NO^{13,15b} is used to form state-selected NO⁺(X¹Σ⁺,*v*) with high purity (>90% for *v* = 0 and 1,¹⁶ >97% and >91% for *v* = 2 and 3, respectively,¹¹ >80% for *v* = 4 and 5¹⁷). Ions are trapped due to the presence of the magnetic field (1.2 T) and the positive electric potential applied to the cell trapping plates (+1.5 V on trapping and 0.0 V on transmitter and receiver plates). Neutral NO molecules pulsed into the cell are pumped away within a fraction of a millisecond.^{15b} During a well-defined, variable storage time NO⁺ can react with the neutral alkyl halide, which is introduced through a leak valve and is present in the ICR cell at a constant pressure of ~10⁻⁷–10⁻⁶ Torr. After a reaction time in the range of zero to several tens or hundreds of milliseconds the mass spectrum is recorded showing the parent ion NO⁺ and the product ion(s) (swept frequency excitation; V_{p-p} = 25 V/1.85'' cubic cell; 70 kHz–1 MHz; 1 kHz/μs and FT of induced signal, 2 ms acquisition time). A subsequent quench pulse removes all the ions from the cell.

This data cycle is repeated typically 100 times: 10 times with the same reaction time to increase the signal-to-noise ratio and at 10 different reaction times which yields the time dependence of the ion signals. The experiment is in general carried out at three different halide pressures and about three times at each pressure. This whole set of experiments is repeated forming NO⁺(*v*) at different vibrational levels.

The tuning of the FT-ICR instrument was the same for all experiments presented in this work including all calibration experiments. Great care has been taken to form approximately the same number of ions in each experiment.

The detailed data analysis is complex and is discussed in detail in Appendix A. Our strategy is to start as simply as possible on each system, which usually means NO⁺(*v* = 0). This ion has the advantage that all it can do is react with the alkyl halide molecules, and it is easy to determine the reaction rate constant and branching ratios. For *v* > 0, NO⁺(*v*) can be collisionally quenched and/or emit an infrared photon in addition to reacting. Hence things become more complicated quickly. Substantial simplification occurs in the analysis because we have previously measured the radiative lifetimes of NO⁺(*v* = 1–5),¹³ and we have measured the reaction rate constants for *v* = 0 with care. By building up from *v* = 0 to *v* = 1 and beyond, we can unambiguously obtain quenching rate constants and reaction rate constants for *v* ≤ 5 in most instances.

Finally, detailed analysis of the sources of error in the experiment must be made. These are given in Appendix B.

Results

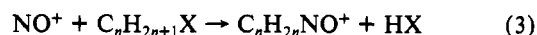
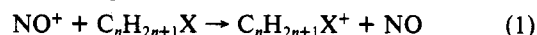
The results are summarized in Tables I, II, and III along with some thermochemical data (where known) and some reaction efficiencies, based on the average dipole orientation (ADO)

TABLE I: Rate Constants, Reaction Efficiencies (*f*_{exp}, *f*_{stat}), and Reaction Enthalpies (Δ*H*_r^o) for Charge-Transfer and Vibrational Quenching Reactions of NO⁺(*v*) with CH₃X and C₂H₅X

	<i>v</i>	rate constants (10 ⁻¹⁰ cm ³ /s)		efficiencies %		Δ <i>H</i> _r ^o ₂₉₈ (kcal/mol)
		<i>k</i> _{rv} ^a	<i>k</i> _{qv} ^b	<i>f</i> _{exp}	<i>f</i> _{stat}	
CH ₃ Cl	0	<<0.01 ^b		0	0	+45.1
	5	<<1 ^b		0	0	+12.5
CH ₃ Br	0	<<0.01 ^b		0	0	+29.6
	4	<0.3 ^c		~0	0	+3.4
CH ₃ I	5	3.3 ± 0.7		19	100	-3.0
	0	<<0.01 ^b		0	0	+6.4
	1	2.3 ± 0.2	14 ± 2	13	70	-0.3
	2	9.2 ± 0.5	7 ± 1 ^d	53	100	-6.9
	3	13 ± 1		74	100	-13.4
C ₂ H ₅ Cl	4	14 ± 1.5		80	100	-19.8
	0	<<0.02 ^b		0	0	+39.3
C ₂ H ₅ Br	5	<<1 ^b		0	0	+6.7
	0	<<0.02 ^b		0	0	+23.6
C ₂ H ₅ I	3	<<0.5 ^b		0	0	+3.8
	4	2.9 ± 0.8	18 ^e	15	~100	-2.6
	5	7 ± 2	13 ^e	36	100	-9.0
	0	0.4 ± 0.2		2	2	+2.0
	1	7.3 ± 0.4	7 ± 1	36	100	-4.7
	2	11.2 ± 0.6	8 ± 1 ^d	55	100	-11.3
	3	16 ± 1.5		79	100	-17.8
	4	16 ± 1.5		79	100	-24.2

^a Charge-transfer rate constant errors are statistical uncertainties accumulated during data analysis. Absolute errors are conservatively estimated to be ^{+50%}/_{-33%}. ^b No products from the reaction were seen. ^c Small signal observed at *m/e* = 94–96, probably due to a small fraction of NO⁺ (*v* = 5) formed by the REMPI process. ^d Average of *k*_{q21} and *k*_{q20}. ^e Not optimized in the fit (see the text). ^f NO⁺ (*v*' → *v*'') vibrational quenching rate constant.

theory.¹⁸ Three reaction channels are observed in the systems discussed here: charge transfer, halide transfer, and formation of a C_nH_{2n}NO⁺ complex



The rate constant for reaction path (i) for NO⁺ in vibrational state *v* is calculated using

$$k_v^{(i)} = x_v^{(i)} k_{rv}$$

where *x*_{*v*}(*i*) is the branching fraction for reaction path (i) and *k*_{rv} is the total reaction rate constant. The overall reaction efficiency *f*_{exp} is the fraction

$$f_{\text{exp}} = k_{rv}/k_{\text{ADO}}$$

This value can be compared to the fraction *f*_{stat} expected from thermochemistry if purely statistical processes are assumed:¹⁵

$$f_{\text{stat}} = \frac{1}{2} e^{-\Delta E/kT} \quad \text{for } \Delta E \geq 0$$

$$f_{\text{stat}} = 1 - \frac{1}{2} e^{\Delta E/kT} \quad \text{for } \Delta E \leq 0$$

The energy difference Δ*E* between products and reactants can be approximated by the reaction enthalpy Δ*H*_r^o₂₉₈ which is calculated from heats of formation.¹⁹

(a) **Methyl and Ethyl Halides.** The only reaction channel observed for NO⁺(*v*) reacting with methyl and ethyl chloride, bromide, and iodide (RX) is charge transfer [reaction 1]. If charge transfer is endoergic, which is true for *v* = 0 in all cases, no products are observed. If the vibrational energy of NO⁺(*v*) is high enough to make reaction 1 exoergic, it turns on. Halide transfer [reaction 2], on the other hand, never turns on (*v* < 6) with methyl and ethyl halides even when thermochemically allowed.

In order to obtain rate constants for a quantitative description of the charge-transfer reactions 1, the following experiments have been carried out. For the NO⁺(*v* = 5) + CH₃Br, NO⁺(*v* = 4) + C₂H₅Br, NO⁺(*v* = 1) + CH₃I, and NO⁺(*v* = 1) + C₂H₅I

TABLE II: Reaction Rate Constants, Reaction Efficiencies (f_{exp}), Branching Ratios (x), and Reaction Enthalpies (ΔH_r°) for^d

$$\text{NO}^+(v) + \text{C}_3\text{H}_7\text{Cl} \begin{cases} \rightarrow \text{C}_3\text{H}_7^+ + \text{ClNO} \\ \rightarrow \text{C}_3\text{H}_6\text{NO}^+ + \text{HCl} \end{cases}$$

	v	total reaction		halide transfer			$\text{C}_3\text{H}_6\text{NO}^+$ formation	
		k_r^a (10^{-10} cm ³ /s)	f_{exp} (%)	x^c	k (10^{-10} cm ³ /s)	ΔH_r° (kcal/mol)	x^c	k (10^{-10} cm ³ /s)
<i>i</i> -C ₃ H ₇ Cl	0	3.6 ± 0.2	17	0.10	0.4	+2.8	0.90	3.2
	1	11.2 ± 1	54	0.55	6.2	-3.9	0.45	5.0
	2	12. ± 1.5	57	0.75	9.0	-10.5	0.25	3.0
<i>n</i> -C ₃ H ₇ Cl	3	10 ± 1.7	48	0.85	8.5	-17.0	0.15	1.5
	0	0.57 ± 0.06	2.7	0.10	0.06	-0.2	0.90	0.51
	1	0.53 ^b	2.5	0.45 ± 0.15	0.24	-6.9	0.55 ± 0.15	0.29
	2	0.68 ^b	3.3	0.70	0.48	-13.5	0.30	0.20
	3	1.12 ^b	5.4	0.80	0.90	-20.0	0.20	0.20
	4	1.41 ^b	6.7	0.98 ± 0.02	1.4	-32.8	0.02 ± 0.02	0.03
	5	<4						

^a Errors given are statistical errors and uncertainties added and accumulated during data analysis. Possible systematic errors are estimated to be $\pm 50\%$. ^b Rate constant determined by the best fit excluding quenching. See Appendix C. ^c Reaction branching ratio. Errors are ± 0.1 unless otherwise specified. ^d For further explanations see the text.

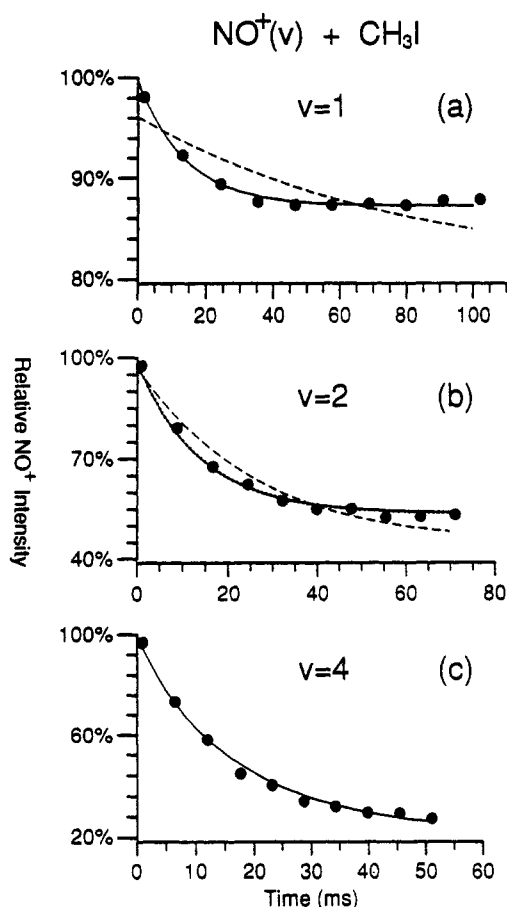
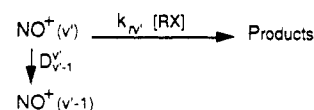


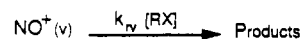
Figure 1. Best fits (lines) to experimental data (dots) of $\text{NO}^+(v) + \text{CH}_3\text{I}$. (a) $\text{NO}^+(v)$ prepared in $v = 1$. Fits based on Scheme I. Dashed line: k_{r1} only is optimized, k_{q10} set to zero. Solid line: both k_{r1} and k_{q10} are optimized. (b) $\text{NO}^+(v)$ prepared in $v = 2$. Fits based on Scheme V. Dashed line: k_{r2} only is optimized, k_{q21} and k_{q20} are set to zero. Solid line: both k_{r2} and k_{q21} are optimized, k_{q20} is set to zero. Dotted line (on top of solid line): both k_{r2} and k_{q20} are optimized, k_{q21} is set to zero. (c) $\text{NO}^+(v)$ prepared in $v = 4$. Fit based on Scheme III, k_{r4} and k_{q40} are optimized. Note the scales are different in all three figures.

systems, state-selected $\text{NO}^+(v = 5)$, $\text{NO}^+(v = 4)$, $\text{NO}^+(v = 1)$, and $\text{NO}^+(v = 1)$, respectively, have been formed by REMPI and the data analyzed using fits based on Scheme I where D_{v-1}^c is the sum of the radiative and quenching rate constants from $\text{NO}^+(v)$ to $\text{NO}^+(v-1)$ (see Appendix A). For all these cases it turned out that in order to get a good fit to the experimental data,

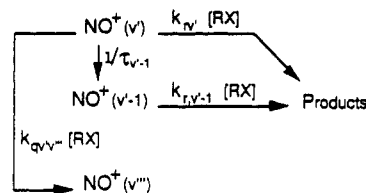
SCHEME I



SCHEME II



SCHEME III



quenching cannot be neglected. This is demonstrated in Figure 1a for the example $\text{NO}^+(v = 1) + \text{CH}_3\text{I}$. If the quenching rate constant k_{q10} is set to zero, the best fit does not match the experimental data. On the other hand, if both k_{r1} and k_{q10} are optimized the fit is very good. Simulations show, in fact, that the shape of the calculated $[\text{NO}^+]$ curve significantly depends on the values of both k_{r1} and k_{q10} .

In the case of $\text{NO}^+(v = 4) + \text{C}_2\text{H}_5\text{Br}$ the quality of the data does not allow simultaneous optimization of two parameters. Therefore the quenching rate is kept constant while k_{r4} is optimized. Good agreement with experimental data is only achieved when the quenching rate constant is set to a large value (Table I). The analysis of the $\text{NO}^+(v = 5) + \text{CH}_3\text{Br}$ data is even more difficult, and no value for quenching could be determined.

Experiments with $\text{C}_2\text{H}_5\text{Br}$, in which $\text{NO}^+(v)$ is state-selectively formed in the $v = 5$ level, are analyzed using Scheme V in Appendix A ($v' = 5$, $v'' = 4$, $v''' \leq 3$) to obtain a charge-transfer rate constant. The $\text{NO}^+(v = 2) + \text{CH}_3\text{I}$ and $\text{C}_2\text{H}_5\text{I}$ systems are dealt with analogously. Again, better fits are obtained when collisional quenching of $\text{NO}^+(v)$ is included. Models with quenching by one (k_{q21} optimized) or by two vibrational quanta (k_{q20} optimized) fit the data well.

The $\text{NO}^+(v = 3) + \text{CH}_3\text{I}$ and $\text{C}_2\text{H}_5\text{I}$ systems are first analyzed by fitting a simple exponential function to data taken at short reaction times when most of the NO^+ ions still are in the $v = 3$ level. The result compares reasonably well with a more sophisticated model based on Scheme III ($v' = 3$, $v'' = 0$). The $\text{NO}^+(v = 4) + \text{CH}_3\text{I}$ and $\text{C}_2\text{H}_5\text{I}$ data are treated the same way. Figure 1c shows that the Scheme III model fits the methyl iodide data very well even for a rather long reaction time of 50 ms. A compilation of the $\text{NO}^+(v) + \text{CH}_3\text{I}$ data analysis is given in Table

TABLE III: Rate Constants, Reaction Efficiencies (f_{exp}), Branching Ratios (x), and Reaction Enthalpies (ΔH_r°) for^c

$$\text{NO}^+(v) + \text{C}_3\text{H}_7\text{X} \begin{cases} \rightarrow \text{C}_3\text{H}_7\text{X}^+ + \text{NO} \\ \rightarrow \text{C}_3\text{H}_7^+ + \text{XNO} \end{cases} \quad \text{X = Br, I}$$

	total reaction			charge transfer			halide transfer		
	v	k_{rv}^a (10^{-10} cm ³ /s)	f_{exp} (%)	x^b	k (10^{-10} cm ³ /s)	ΔH_r° , ₂₉₈ (kcal/mol)	x^b	k (10^{-10} cm ³ /s)	ΔH_r° , ₂₉₈ (kcal/mol)
<i>i</i> -C ₃ H ₇ Br	0	17.6 ± 0.9	85	0	0	+18.9	1	17.6	-1.0
	1	17.8 ± 1.1	86	0	0	+12.2	1	17.8	-7.7
	2	16.7 ± 1.3	80	0	0	5.6	1	16.7	-14.3
	3	17.8 ± 1.5	86	0.03 ± 0.01	0.5	-0.9	0.97 ± 0.01	17.3	-20.8
<i>n</i> -C ₃ H ₇ Br	0	11.4 ± 0.6	55	0	0	+20.7	1	11.4	-4.2
	1	9.0 ± 0.7	43	0	0	+14.0	1	9.0	-10.9
	2	10.1 ± 0.8	49	0	0	+7.4	1	10.1	-17.5
	3	9.9 ± 0.9	48	0	0	+0.9	1	9.9	-24.0
<i>i</i> -C ₃ H ₇ I	0	12.5 ± 1.1	60	0.25	3.1	-5.5	0.75	9.4	-30.4
	1	16.5 ± 0.9	78	0.15	2.5	-1.6	0.85	14	
	2	17.5 ± 1.1	83	0.35	6.1	-8.3	0.65	11	
	3	16.0 ± 1.3	76	0.35	5.6	-14.9	0.65	10	
<i>n</i> -C ₃ H ₇ I	0	25.0 ± 1.8	118	0.20	5.0	-21.4	0.80	20	
	1	22.5 ± 2.1	107	0.15	3.4	-27.8	0.85	19	
	2	17.5 ± 0.9	83	0.03 ± 0.01	0.5	+0.29	0.97 ± 0.01	17	
	3	14.3 ± 1.1	68	0.35	5.0	-6.4	0.65	9	
	2	18.3 ± 1.3	87	0.40	7.3	-13.0	0.60	11	
	3	22.0 ± 1.7	104	0.25	5.5	-19.5	0.75	17	
	4	19.5 ± 1.9	92	0.10	2.0	-25.9	0.90	18	

^a Errors given are statistical errors, uncertainties added, and accumulated during data analysis. Maximum systematic errors estimated at ^{+50%}.

^b Reaction branching ratio. Errors for $x = 0$ and $x = 1$ are less than ± 0.01 , else ± 0.1 unless otherwise specified. ^c For further explanations see the text.

TABLE IV: Parameters Used in the Fit to the NO⁺(v) + CH₃I Data^a

v	model	v'''	v''	v'	$\tau_{v''}$	$\tau_{v'}$	$k_{\text{rv}''}$	$k_{\text{rv}'}$	k_{rv}	$k_{\text{qv}''}$	$k_{\text{qv}'}$	k_{qv}
1	Scheme I		0	1		90		0	<i>0.54</i>		0	
1	Scheme I		0	1		90		0	<i>2.3</i>		<i>14</i>	
2	Scheme V	0	1	2	90	45	0	2.3	<i>5.6</i>	14	0	0
2	Scheme V	0	1	2	90	45	0	2.3	<i>9.2</i>	14	<i>8.6</i>	0
2	Scheme V	0	1	2	90	45	0	2.3	<i>9.2</i>	14	0	<i>6.3</i>
4	Scheme II			4					<i>12</i>			
4	Scheme III	0	3	4	31	24	0	13	<i>14</i>			<i>4</i>

^a The initial vibrational state of NO⁺(v) formed by REMPI is called v . The vibrational levels used in the model are called v' , v'' , v''' . Optimized parameters are in ***bold face italic***. Rate constants in 10^{-10} cm³ s⁻¹, radiative lifetimes τ in ns.

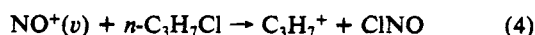
TABLE V: Standard Reaction Enthalpies and Observed Rate Constants for Reaction as a Function of the Vibrational Excitation (v) in NO
$$\text{NO}^+(v) + n\text{-C}_3\text{H}_7\text{Cl} \begin{cases} \rightarrow \text{CH}_3\text{CH}_2\text{CH}_2^+ + \text{ClNO} \text{ (a)} \\ \rightarrow \text{CH}_3\text{CH}^+\text{CH}_3 + \text{ClNO} \text{ (b)} \\ \rightarrow [\text{cyclo-C}_3\text{H}_6\text{H}]^+ + \text{ClNO} \text{ (c)} \end{cases}$$

v	ΔH_r° , _{298K} (kcal mol ⁻¹)			k (10^{-11} cm ³ s ⁻¹)
	a ^a	b	c	
0	+19.9	-0.2	+7.4	0.6
1	+13.2	-6.9	+0.7	2.4
2	+6.6	-13.5	-5.9	4.8
3	+0.1	-20.0	-12.4	9.0
4	-6.3	-26.4	-18.8	14

^a Although CH₃CH₂CH₂⁺ is not a stable structure, thermochemical data have been obtained by photoelectron spectroscopy studies of the stable radical CH₃CH₂CH₂[•].³⁶ The CH₃CH₂CH₂⁺ ion rearranges to [cyclo-C₃H₆H]⁺ with no activation barrier.³⁷

IV. The summary of all the final results is presented in Table I.

(b) *n*-Propyl and Isopropyl Chloride. NO⁺ reacting with *n*-propyl chloride yields two product ions C₃H₇⁺ and C₃H₆NO⁺. Both channels are slow with or without vibrational excitation of NO⁺ ($k \leq 10^{-10}$ cm³ s⁻¹). The total reaction efficiency is only a few percent. The halide transfer reaction

TABLE VI: Thermochemical Data for the Reaction NO⁺ + C₃H₇X → C₃H₆NO⁺ + HX^a

X	C ₃ H ₇ X	ΔH_f° (C ₃ H ₇ X)	ΔH_f° (HX)	ΔH_f° (HX) - ΔH_f° (C ₃ H ₇ X)
Cl	<i>i</i> -C ₃ H ₇ Cl	-34.6 ± 0.1	-22.1 ± 0.04	12.5
	<i>n</i> -C ₃ H ₇ Cl	-31.6 ± 0.1		9.5
Br	<i>i</i> -C ₃ H ₇ Br	-23.4 ± 0.2	-9	14.4
	<i>n</i> -C ₃ H ₇ Br	-20.2 ± 0.1		11.2
I	<i>i</i> -C ₃ H ₇ I	-9.9 ± 0.4	-6.3 ± 0.05	16.2
	<i>n</i> -C ₃ H ₇ I	-7.8 ± 0.4		14.1

^a Heat of formations (ΔH_f°) at 298 K in kcal/mol.¹⁹

is observed for $v \geq 0$. For $v = 0$, reaction 4 is exothermic only if the C₃H₇⁺ product has the structure (CH₃CHCH₃)⁺ (Table V). Consequently, rearrangement in the [NO-C₃H₇Cl]⁺ collision complex must be involved. For NO⁺($v \geq 2$) formation of protonated cyclopropane is also exothermic. It is interesting to note that there is a continuous increase of the rate constant from $\sim 6 \times 10^{-12}$ cm³ s⁻¹ for $v = 0$ to $\sim 10^{-10}$ cm³ s⁻¹ for $v = 4$. That is, no "threshold" is observed when the protonated cyclopropane form of C₃H₇⁺ is reached.

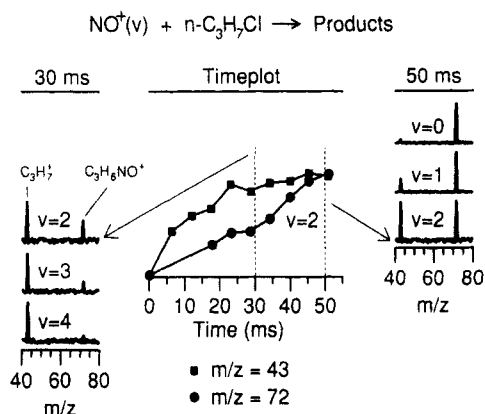
The mechanism of the other reaction channel



is rather complex, resulting in elimination of HCl and leaving C₃H₆NO⁺ ($m/z = 72$). Using labeled ¹⁵N¹⁸O yielded the corresponding ion at $m/z = 75$ confirming the formation of

TABLE VII: Total Rate Constants ($10^{-9} \text{ cm}^3 \text{ s}^{-1}$) for Calibration Reactions To Determine the Error in Absolute Pressure Measurements^d

	this work	previous work		
		ICR studies ^a	other work ^b	av
$\text{C}_3\text{H}_4^+ + \text{C}_3\text{H}_4^c$	0.71	1.1	0.59, 0.37, 0.64	0.68
$\text{Ar}^+ + \text{CO}_2$	0.39	0.42, 0.46, 0.42	0.76, 0.55, 0.7, 0.55, 0.56, 0.44	0.54
$\text{CO}^+ + \text{CO}_2$	1.34	3.7, 0.96	1.4, 1.0, 1.1	1.63
$\text{N}_2^+ + \text{CO}_2$	0.86	0.55	0.77, 0.9, 0.8	0.77

^a Reference 38 or refs 39–45 from left to right and top to bottom.^b Reference 38 or refs 46–60 from left to right and top to bottom.^c $\text{CH}_2=\text{C}=\text{CH}_2^+ + \text{CH}_2=\text{C}=\text{CH}_2$. ^d In this work experiments were carried out in the pressure range of 10^{-7} – 10^{-6} Torr using electron impact ionization for ion formation. The same electron energy was used as in previous ICR studies^{39–45} or 40 eV if not indicated there.**Figure 2.** Observed branching ratios for C_3H_7^+ ($m/z = 43$) and $\text{C}_3\text{H}_6\text{NO}^+$ formation ($m/z = 72$) in the $\text{NO}^+(v) + n\text{-C}_3\text{H}_7\text{Cl}$ system. $\text{NO}^+(v)$ is initially prepared in the vibrational level indicated in the figure but relaxes (see Scheme IV) during reaction time to lower vibrational states. This is apparent in the timeplot for $v = 2$ where the observed branching ratio at short times is determined by the $v = 2$ branching ratio but as time proceeds also by the $v = 1$ and $v = 0$ branching ratios.

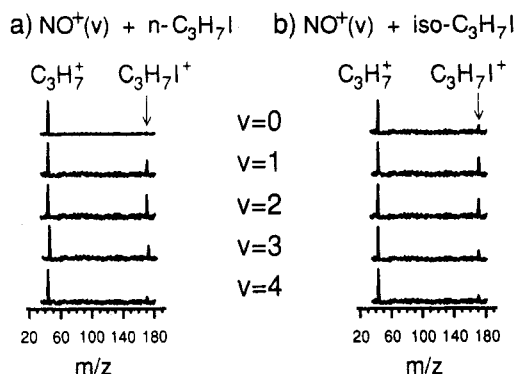
$\text{C}_3\text{H}_6\text{NO}^+$. Williamson and Beauchamp¹⁴ observed analogous reactions for NO^+ reacting with isopropyl fluoride and chloride. The rate constant for HCl elimination decreases with increasing vibrational excitation of $\text{NO}^+(v)$, with chloride transfer becoming dominant for $\text{NO}^+(v \geq 2)$ (Figure 2).

The same two product ions, C_3H_7^+ and $\text{C}_3\text{H}_6\text{NO}^+$, are observed in the reaction of $\text{NO}^+(v)$ with isopropyl chloride, but the reactivity is about an order of magnitude higher. The total reaction efficiency still is only 50% or less, however. Chloride transfer from $\text{iso-C}_3\text{H}_7\text{Cl}$ to $\text{NO}^+(v)$ is only exothermic for $v \geq 1$ and is the dominant channel for $v > 2$. Perhaps this is why $\text{C}_3\text{H}_6\text{NO}^+$ formation is much faster at low v than in the corresponding reaction with n -propyl chloride, although structural rearrangement in the transition states could also contribute to this result.

Charge transfer [reaction 1] from $\text{NO}^+(v < 6)$ to $\text{C}_3\text{H}_7\text{Cl}$ is endoergic for both n -propyl and isopropyl chloride and has not been observed.

Quantitative analysis of the experimental data yields the rate constants and branching ratios summarized in Table II. Sorting out the effect of quenching on the rate constants is difficult in these cases and is discussed in detail in Appendix C. Quenching can have a big effect on the determination of branching ratios for reactions with $v > 0$. To minimize the uncertainty, branching ratios were determined from data at short reaction times when most of $\text{NO}^+(v)$ was still in the initial vibrational level. This method was not possible, however, for very slow reactions and very small branching ratios. Therefore some branching ratios listed in Table II have a relatively large error.

(c) *n*-Propyl and Isopropyl Bromide and Iodide. The dominant channel for $\text{NO}^+(v)$ reacting with $\text{C}_3\text{H}_7\text{Br}$ and $\text{C}_3\text{H}_7\text{I}$ is halide transfer for both propyl isomers and both halides. All reactions

**Figure 3.** Branching ratios for C_3H_7^+ ($m/z = 43$) and $\text{C}_3\text{H}_7\text{I}^+$ formation ($m/z = 170$) in the (a) $\text{NO}^+(v) + n\text{-C}_3\text{H}_7\text{I}$ and (b) $\text{NO}^+(v) + i\text{-C}_3\text{H}_7\text{I}$ system, observed after 10-ms reaction time, as a function of the initial vibrational state of $\text{NO}^+(v)$.

are fast, close to the collision limit. Charge transfer is observed as a second path when exoergic.

The reaction



has three different C_3H_7^+ isomers to be considered. Initial formation of $\text{CH}_3\text{CH}_2\text{CH}_2^+$ is endothermic for $v \leq 2$. Since C_3H_7^+ formation is observed for $v = 0, 1$, and 2 , rearrangement must take place in the reaction intermediate. There is no significant increase in the rate of C_3H_7^+ formation going from $\text{NO}^+(v = 2)$ to $\text{NO}^+(v = 3)$ indicating initial formation of $\text{CH}_3\text{CH}_2\text{CH}_2^+$ is probably not important. The reaction efficiency stays around 50% for $v = 0$ – 4 . Bromide transfer is much faster than the corresponding chloride transfer; ~ 200 times for $v = 0$ and ~ 10 times faster for $v = 4$. Charge transfer from $\text{NO}^+(v)$ to $n\text{-C}_3\text{H}_7\text{Br}$ is exoergic for $v \geq 4$ and is in fact observed for $v = 4$ with a branching ratio of about 25%.

The chemistry of $\text{NO}^+(v)$ with isopropyl bromide is mostly the same as with n -propyl bromide. Charge transfer is observed when energetically allowed, but it always is the less important channel compared to the predominant bromide transfer reaction. The total rate constants are a little closer to the collision limit than those of n -propyl bromide.

Collisions between $\text{NO}^+(v)$ and both n -propyl and isopropyl iodide are almost 100% efficient for all values of v , forming $\text{C}_3\text{H}_7\text{I}^+$ and C_3H_7^+ as ionic products. However, vibrational excitation of $\text{NO}^+(v)$ has a remarkable effect on the branching ratio (Figure 3). Charge transfer is small for $v = 0$, increases dramatically for $v = 1$ and 2 , and then decreases for $v = 3$ and 4 . The ionization potential of n -propyl iodide is slightly (0.005 eV) higher than that of NO which explains the comparably small branching ratio for $\text{NO}^+(v = 0) + n\text{-C}_3\text{H}_7\text{I}$ charge transfer. However, the dynamics of these reactions must be very interesting for such a bizarre product dependence to be observed. Perhaps in this case C_3H_7^+ formation is exothermic enough for high v values to access another mechanism, such as $[\text{cyclo-C}_3\text{H}_6]\text{H}^+$ formation from $n\text{-C}_3\text{H}_7\text{I}$.

$\text{C}_3\text{H}_6\text{NO}^+$ is not observed with propyl bromides and iodides. In fact, the reaction becomes energetically less favorable when moving from Cl to Br to I (Table VI) in contrast to charge transfer and halide transfer.

Rate constants and branching ratios summarized in Table III have been obtained applying the same concepts outlined in the previous section about propyl chloride. Since the rate constants for reaction are close to the collision limit, vibrational quenching of $\text{NO}^+(v)$ by collisions is of minor importance here, and the accuracy for the different k_r determined is much higher than in the n -propyl chloride case, as is demonstrated in Figure 4 for the example of $\text{NO}^+(v = 1) + \text{iso-C}_3\text{H}_7\text{Br}$. All propyl bromide and iodide data could be fit well by models excluding quenching.

Discussion

(a) **Quenching.** If no chemical reaction results from a collision of a vibrationally excited $\text{NO}^+(v)$ with another particle, the

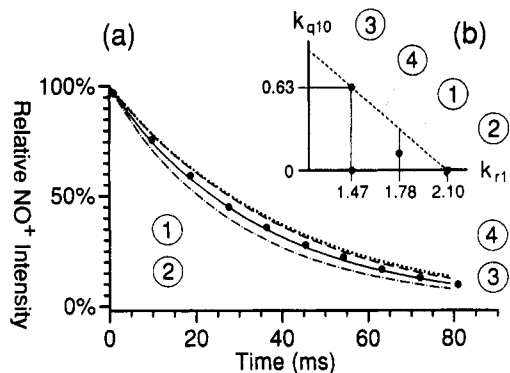


Figure 4. (a) Simulations (lines) along with experimental data (dots) for the $\text{NO}^+(v=1) + i\text{-C}_3\text{H}_7\text{Br}$ system. Values for the parameter pair (k_{r1}, k_{q10}) used in the simulations 1–4 are shown in diagram (b). k_{r1} obviously can accurately be determined, whereas k_{q10} is undeterminable (compare, e.g., simulations 3 and 4). The dashed line in (b) represents the collision limit $k_{r1} + k_{q10} = 2.1 \times 10^{-9} \text{ cm}^3 \text{ s}^{-1}$. $k_{r0} = 1.76 \times 10^{-9} \text{ cm}^3 \text{ s}^{-1}$.

question is whether the vibrational energy of NO^+ after the collision is still the same as before. If vibrational quenching is present, the second question is, how much of the internal energy decreases in one collision.

The first question can unambiguously be answered for some systems presented in this work. The methyl and ethyl bromide and iodide data is most suitable to get information about quenching of $\text{NO}^+(v)$ as outlined in the results section, so our discussion is limited to these systems. In all these cases collisional quenching of $\text{NO}^+(v)$ is a major process, with rate constants as high as $1.4 \times 10^{-9} \text{ cm}^3 \text{ s}^{-1}$ for the $\text{NO}^+(v=1) + \text{CH}_3\text{I}$ and $1.8 \times 10^{-9} \text{ cm}^3 \text{ s}^{-1}$ for the $\text{NO}^+(v=4) + \text{C}_2\text{H}_5\text{Br}$ system (Table I). On the basis of the information available it can be concluded that almost every collision which does not yield products leads to $\text{NO}^+(v)$ quenching, since the sum of the rate constants for charge transfer and quenching is always about equal to the rate constant for collision. In our experiments quenching of $\text{NO}^+(v)$ becomes visible only by competition with a chemical reaction. Consequently, when chemical reactivity is very slow, or zero, quenching cannot be investigated.

The high rates for vibrational quenching of $\text{NO}^+(v)$ by alkyl halides is in general agreement with the measurements of Morris et al.¹⁰ who obtained a value of $6.5 \times 10^{-10} \text{ cm}^3 \text{ s}^{-1}$ for $(v > 0) \rightarrow (v = 0)$ quenching in the $\text{NO}^+ + \text{CH}_3\text{Br}$ system. High quenching efficiencies have generally been observed in ion-polar neutral collisions,^{3,8,10} and a rough correlation between the polarizability (and/or dipole moment) of the neutral and the quenching probability is evident. To explain the strong influence of the electrostatic interaction on quenching, Ferguson and co-workers^{3,8,20} suggested a model in which vibrational relaxation occurs by vibrational predissociation of the transient collision complex which competes with unimolecular decay back to the original reactants. A measure of the probability of this latter process is the lifetime of the collision complex which is strongly related to the depth of the potential well of the ion-neutral complex and thus to the electrostatic interactions between ion and neutral.

A quenching model which includes conversion of vibrational to rotational energy cannot be excluded and has been suggested²¹ to explain enhanced quenching probabilities for vibrationally excited neutrals with H-atom containing quenchers.

The second question, whether $\text{NO}^+(v)$ is quenched by one or more vibrational quanta per collision, can only partly be answered by the experimental data available. Figure 1b shows that a model including sequential $(v=2) \rightarrow (v=1)$ and $(v=1) \rightarrow (v=0)$ quenching of $\text{NO}^+(v)$ fits the data equally well with one assuming $(v=2) \rightarrow (v=0)$ quenching. Therefore the data is not conclusive whether one of the two quenching processes is dominant or whether it is a combination of the two. In some earlier work^{11,13} about radiative lifetime measurements of $\text{NO}^+(v)$, methyl iodide was employed as a "monitor" of both $\text{NO}^+(v=1)$ and $\text{NO}^+(v=2)$. The fact that the measurement of the $\text{NO}^+(v=2)$ concentration was not hindered by the presence of $\text{NO}^+(v=1)$ was explained

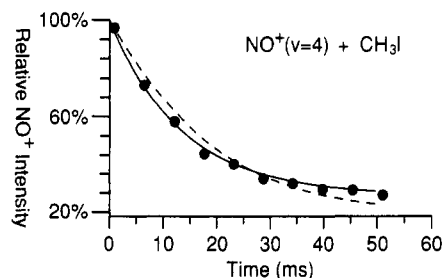


Figure 5. Simulations (lines) based on Scheme IV along with experimental data (dots) for the $\text{NO}^+(v=4) + \text{CH}_3\text{I}$ system. The parameters k_{r0} , k_{r1} , k_{r2} , k_{r3} , and k_{q10} are set to the values shown in Table I. The dashed line is obtained when sequential quenching of $\text{NO}^+(v)$ is assumed (values in $10^{-9} \text{ cm}^3 \text{ s}^{-1}$): $k_{r4} = 1.0$, $k_{q21} = 0.86$ (Table IV), $k_{q32} = 0.6$, $k_{q43} = 0.9$, $k_{qv'v''} = 0$ if $v'' \neq v' - 1$. The solid line represents $(v') \rightarrow (v'' = 0)$ quenching: $k_{r4} = 1.4$, $k_{q20} = 0.63$ (Table IV), $k_{q30} = 0.4$, $k_{q40} = 0.4$, $k_{qv'v''} = 0$ if $v'' \neq 0$.

by the considerably lower charge-transfer reactivity and higher quenching probability of $\text{NO}^+(v=1)$ compared to $\text{NO}^+(v=2)$. On the other hand it could also indicate that $\text{NO}^+(v=2)$ is directly quenched to $v=0$. Further investigations should clarify this point.

Some support for the $(v') \rightarrow (v'' = 0)$ quenching model is supplied by the $\text{NO}^+(v=4) + \text{CH}_3\text{I}$ data shown in Figure 1c together with a good fit including $(v=4) \rightarrow (v=0)$ quenching. To clarify whether the fitting model represents reality or just coincidentally fits the experimental data, two different simulations, one including $(v) \rightarrow (v-1)$ quenching only and one employing the other extreme $(v') \rightarrow (v'' = 0)$ quenching only, are compared with each other (Figure 5). The quenching rate constants assumed in the simulations all have reasonable values. Although the two quenching models yield similar results, the second model (solid line in Figure 5) agrees better with the data, indicating that quenching of more than one vibrational quantum per collision is at least partly present. The physical meaning of k_{q40} resulting from the fit shown in Figure 1c is not necessarily clear. It could in fact be the rate constant for $(v=4) \rightarrow (v=0)$ quenching, but it also could be just some optimized fitting parameter without direct physical interpretation if sequential $(v) \rightarrow (v-1)$ quenching is partly involved.

The idea of quenching by more than one quantum per collision is not compatible with the vibrational \rightarrow translational quenching model suggested by Böhringer et al.³ which is based on a mechanism including vibrational predissociation of the transient collision complex. Detailed experimental and theoretical studies on vibrational predissociation have been performed for neutral van der Waals molecules which indicate that transfer of more than one vibrational quantum of energy from a chemical bond to the van der Waals bond is possible but not predominant.^{22,23} We are currently in the process of designing specific experiments that should unambiguously address this interesting and important point.

(b) Charge Transfer. The adiabatic ionization potential of NO is lower than all but isopropyl iodide of the alkyl halides considered here. This means that charge transfer from $\text{NO}^+(v=0)$ to the alkyl halides is generally endoergic and therefore generally not observed. In all cases, however, charge transfer is observed as soon as the internal energy of $\text{NO}^+(v)$ is large enough to make the process exoergic. Thus, the vibrational energy of $\text{NO}^+(v)$ is utilized to turn on the reaction, to help the electron hop from the alkyl halide to the NO^+ ion. The correctness of this turn on principle has been assumed^{7-10,12} for many years as part of the monitor technique (see Introduction), but our result is direct experimental evidence for it. However, our studies clearly show that the "switch to turn on" charge transfer is not of the "on/off"-type but "continuous", a factor which has not been considered in the turn on assumption.^{7-10,12} It has always been assumed that an exoergic charge-transfer process is very fast, near the collision limit, but this is not necessarily the case. In fact, in all the systems studied here exothermicity of one quantum or less of vibrational energy in $\text{NO}^+(v)$ is not enough to observe a very fast charge transfer. CH_3I^+ , for example, is formed rather slowly in the

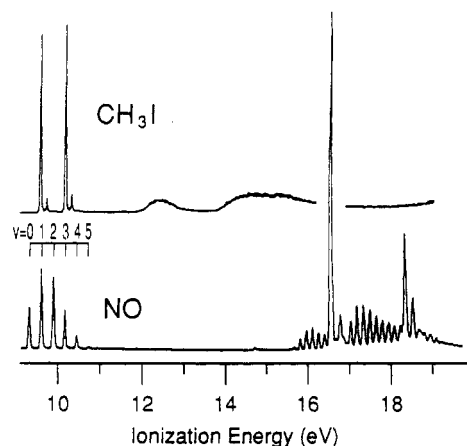


Figure 6. He I photoelectron spectra of CH_3I and NO .²⁶ The “ v ” assignments belong to the $\text{NO}^+(\text{X}^1\Sigma^+, v) \leftarrow \text{NO}(\text{X}^2\Pi, v = 0)$ transition. The CH_3I spectrum is a typical representative for all alkyl halide spectra.

$\text{NO}^+(v = 1) + \text{CH}_3\text{I}$ system ($2.3 \times 10^{-10} \text{ cm}^3 \text{ s}^{-1}$). In some earlier studies^{11,13} the same observation had already been made qualitatively. The derivation of the estimated rate constant of $(1.3 \pm 1.0) \times 10^{-10} \text{ cm}^3 \text{ s}^{-1}$ given there was based on a comparison of the CH_3I^+ signals after long reaction times in the $\text{NO}^+(v = 1)$ and $\text{NO}^+(v = 2) + \text{CH}_3\text{I}$ systems. Quenching of $\text{NO}^+(v)$ was obviously not considered in this method of analysis. Taking this difference of data analysis into account, our result compares very well with the earlier value [for comparison see also Figure 1a and Table IV].

In the cases of methyl and ethyl iodide, increasing the exoergicity for charge transfer by increasing the vibrational energy in $\text{NO}^+(v)$ drives the process faster, eventually close to the collision limit. For some simple charge-transfer reactions it has been suggested²⁴ that the electron jump is quick compared to nuclear motion and that the Franck-Condon factors for the electronic transitions involved may control charge-transfer rates. Indeed, charge transfer in $\text{H}_2^+(v) + \text{Ar}, \text{N}_2, \text{CO}, \text{O}_2$, performed with state-selected $\text{H}_2^+(v)$, could be understood quite well using a Franck-Condon type analysis.²⁵ Figure 6 shows the photoelectron spectra of methyl iodide and nitric oxide. It can be seen that the Franck-Condon factor for the transition from the neutral ground state to the ionic ground state in CH_3I is very favorable, whereas the overlap of the $\text{NO}(\text{X}^2\Pi, v = 0)$ vibrational wave function with the various $\text{NO}^+(\text{X}^1\Sigma^+, v)$ wave functions peaks at $v = 1$ or 2 due to different equilibrium bond lengths in the two electronic states. It also can be seen that charge transfer from $\text{NO}^+(v = 1)$ to CH_3I is slightly exoergic if the $\text{NO}^+(\text{X}^1\Sigma^+, v = 1) \rightarrow \text{NO}(\text{X}^2\Pi, v = 0)$ transition is involved. Transitions to $\text{NO}(\text{X}^2\Pi, v > 0)$ would not provide enough energy to ionize CH_3I . For $\text{NO}^+(v = 2) + \text{CH}_3\text{I}$ charge transfer, though, there are two possible vibronic transitions ($\text{X}^1\Sigma^+, v = 2 \rightarrow \text{X}^2\Pi, v = 0, 1$) supplying enough energy for CH_3I ionization [ground-state vibrational frequencies:²⁷ $\omega_e(\text{NO}^+) = 2377 \text{ cm}^{-1}$, $\omega_e(\text{NO}) = 1904 \text{ cm}^{-1}$]. Thus, the increasing number of possible vibronic $\text{NO}^+ \rightarrow \text{NO}$ transitions with increasing vibrational excitation in $\text{NO}^+(v)$ might explain the simultaneous increase in the charge transfer rate constant.

Other models have been proposed to explain vibrational effects on charge-transfer rates, including complex formation. In this case the complex lifetime, which determines the charge-transfer probability, may be enhanced by vibrational excitation of the ions. Durup-Ferguson et al.²⁸ found that excitation of the bending vibration in a number of molecular ions increases the efficiency for charge transfer with various neutral molecules. They reasoned that the angular momentum of the bending vibration in the ion and angular momentum resulting from the orbiting motion of ion and neutral might couple and thus transfer energy from orbital to internal motion, which would stabilize the complex. According to this model, excitation of stretch vibrations should have little or no influence on the charge-transfer probability, which is true in the case of $\text{N}_2^+(v) + \text{O}_2$ ²⁹ but is not true in the case of $\text{NO}^+(v) + \text{NH}_3$ ¹⁷ and for $\text{NO}^+(v)$ + alkyl halides reported here. Increasing

v in the stretch vibration enhances the charge-transfer probability in these latter systems. Other results of charge-transfer studies with state-selected ions^{6b,30} cannot be explained entirely with the model proposed by Durup-Ferguson et al.²⁸ Hence, the evidence suggests there are most likely different charge-transfer mechanisms predominant for different ion-molecule pairs at near thermal energies.

The charge-transfer efficiency in the $\text{NO}^+(v) + n$ -propyl and isopropyl iodide systems reaches a maximum and drops again with increasing vibrational excitation of $\text{NO}^+(v)$ (Figure 3) as opposed to $\text{NO}^+(v) +$ methyl and ethyl iodide where it stays high at high values of v . Since in the propyl iodide cases charge transfer has to compete with halide transfer, the decrease in charge transfer at high v might be due to an iodide transfer effect (see next section).

(c) Halide Transfer. Halide transfer from an alkyl halide to $\text{NO}^+(v = 0)$ is significantly exothermic for $\text{C}_3\text{H}_7\text{Br}$ and $\text{C}_3\text{H}_7\text{I}$, where the process is fast and competes successfully with charge transfer. For $\text{C}_3\text{H}_7\text{Cl}$ it is close to thermoneutral and observed as a very slow reaction. For ethyl halides it is endothermic by more than 10 kcal mol⁻¹ and therefore not observed. With increasing vibrational excitation of $\text{NO}^+(v)$ halide transfer stays fast for $\text{C}_3\text{H}_7\text{Br}$ and $\text{C}_3\text{H}_7\text{I}$, gets significantly faster for $\text{C}_3\text{H}_7\text{Cl}$, and still is not observed for ethyl halides even when it is exothermic.

The most instructive information about reactivity change as a function of vibrational energy is obtained from propyl chloride. In the $\text{NO}^+(v = 0) + i\text{-C}_3\text{H}_7\text{Cl}$ system, halide transfer is endothermic by about 2.8 kcal mol⁻¹ and proceeds only slowly with a rate constant in the $10^{-11} \text{ cm}^3 \text{ s}^{-1}$ range (Table II). Increasing the NO^+ vibrational energy by one quantum makes the process exothermic and raises the reactivity by more than an order of magnitude. For $\text{NO}^+(v = 3)$ the rate constant for chloride transfer reaches a value of $\sim 8 \times 10^{-10} \text{ cm}^3 \text{ s}^{-1}$ or 40% of the collision limit. Similar behavior is observed for $n\text{-C}_3\text{H}_7\text{Cl}$ except that all the rates are about ten times lower, even though for $n\text{-C}_3\text{H}_7\text{Cl}$ halide transfer is ~ 3 kcal/mol more exothermic than the comparable $i\text{-C}_3\text{H}_7\text{Cl}$ reaction. This dramatic difference in reactivity must be due to rearrangement in the $[\text{NO}-n\text{-C}_3\text{H}_7\text{Cl}]^+$ collision complex to give $\text{CH}_3\text{CHCH}_3^+ + \text{ClNO}$ products, as energetically required. It can also be concluded that additional vibrational energy in $\text{NO}^+(v)$ increases the chloride transfer reactivity, but that the process is never totally “turned on” like it is with $\text{C}_3\text{H}_7\text{Br}$ and $\text{C}_3\text{H}_7\text{I}$.

There is apparently a small barrier for rearrangement of the collision complex in the $n\text{-C}_3\text{H}_7\text{Br}$ case since the bromide transfer efficiency is reduced by 30–40% compared to $i\text{-C}_3\text{H}_7\text{Br}$ where no rearrangement is required. In the $n\text{-C}_3\text{H}_7\text{Cl}$ case there appears to be a significant barrier to rearrangement in the collision complex since the chloride transfer efficiency is about five to ten times less than that of $i\text{-C}_3\text{H}_7\text{Cl}$. Summarizing, it can be concluded that the barrier for H-atom rearrangement in the collision complex becomes kinetically significant when the reaction enthalpy is near -4 kcal mol^{-1} ($n\text{-C}_3\text{H}_7\text{Br}$ case). In $n\text{-C}_3\text{H}_7\text{Cl}$ the very slow reaction suggests the H-atom rearrangement barrier is very near the energy of the reactants.

The results discussed above might be generally the case for rearrangements in carbonium ions; that is, when energetically allowed, rapid rearrangement takes place in the intermediate complex to form a stable carbonium ion before a less stable carbonium ion can be formed. This interpretation is in line with photoelectron-photoion coincidence^{31,32} and photoionization mass spectrometry³³ studies on n -propyl halides which indicate that fragmentation of these species is accompanied by rearrangement.

Direct formation of $[\text{CH}_2\text{-CH}_2\text{-CH}_2]^+$ becomes thermoneutral or exothermic for $\text{NO}^+(v \geq 3)$ but probably does not occur in either $n\text{-C}_3\text{H}_7\text{Cl}$ or $n\text{-C}_3\text{H}_7\text{Br}$ since no rate acceleration is observed at this value of v . Even in the $\text{NO}^+(v = 5) + n\text{-C}_3\text{H}_7\text{Cl}$ system, where chloride transfer is the sole product, it is slower than in the $\text{NO}^+(v = 1) + i\text{-C}_3\text{H}_7\text{Cl}$ system. This result suggests that the rearrangement barrier in the $n\text{-C}_3\text{H}_7\text{Cl}$ complex effectively blocks product formation.

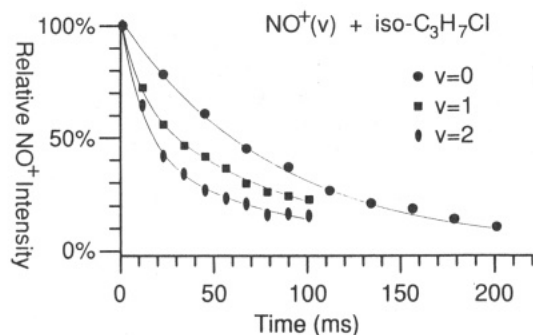


Figure 7. NO⁺ signal as a function of reaction time in the NO⁺(*v*) + *i*-C₃H₇Cl system. NO⁺(*v*) is initially formed in *v* = 0 (circles), *v* = 1 (squares), and *v* = 2 (ovals).

The final conclusions are as follows: Additional vibrational energy in NO⁺(*v*) is only partly utilized to drive halide transfer and in the case of *n*-propyl halide it does not cause the systems to switch to a more straightforward atom abstraction reaction mechanism which opens up from the energetic point of view as vibrational energy in NO⁺(*v*) is increased.

(d) C₃H₆NO⁺ Formation. For thermochemical reasons the channel yielding C₃H₆NO⁺ ions is only observed for the two isomers of propyl chloride. In these cases it is the main product for NO⁺(*v* = 0) even though for *n*-C₃H₇Cl the mechanistically more direct halide transfer channel is energetically accessible. Rate constants are rather small, however (Table II).

Three points are striking in comparing *n*-C₃H₇Cl with *i*-C₃H₇Cl. First, C₃H₆NO⁺ formation is about ten times slower for *n*-C₃H₇Cl independent of the vibrational energy in NO⁺(*v*). Second, for both C₃H₇Cl isomers the rate constants for C₃H₆NO⁺ formation decrease with increasing *v* in NO⁺(*v*). Third, the chloride transfer/C₃H₆NO⁺ formation branching ratios are about the same for both C₃H₇Cl isomers and significantly change in favor of halide transfer with increasing vibrational excitation in NO⁺(*v*). All this means that the chemistry with NO⁺(*v*) is almost exactly the same for *n*-C₃H₇Cl as for *i*-C₃H₇Cl, but it happens about ten times slower. For chloride transfer this difference in reactivity has been associated with the barrier for H-rearrangement in the collision complex which is necessary for *n*-C₃H₇Cl. But since the same difference in reactivity also is observed in C₃H₆NO⁺ formation, the question arises whether there is a common origin. It might be that the same rearrangement barrier as in the chloride transfer channel has to be surmounted before HCl can be eliminated.

Summarizing, C₃H₆NO⁺ formation is only observed for NO⁺(*v*) reacting with *n*-propyl or isopropyl chloride. In these cases it is the main channel for NO⁺(*v* = 0) but diminishes in importance relative to the chloride transfer channel when NO⁺(*v*) is vibrationally excited by two quanta or more.

Conclusions

The chemistry of the nitrosyl ion with alkyl halides is strongly dependent on the degree of vibrational excitation in NO⁺(*v*) under otherwise thermal conditions. Three reaction channels are observed: charge transfer, halide transfer, and C₃H₆NO⁺ formation.

In all cases charge transfer is present as soon as the internal energy of NO⁺(*v*) is sufficient to make the process exoergic. Increasing charge transfer efficiency is usually observed with increasing *v* in NO⁺(*v*) which might be due to Franck-Condon factors for the electronic transitions involved and the increasing number of NO⁺(*v*) → NO(*v*) transitions possible.

Halide transfer is the major reaction channel if it is significantly exothermic for NO⁺(*v* = 0), which is true for propyl bromides and iodides. In these cases the process is rapid even for the *n*-propyl isomers where a rearrangement of the reaction intermediate is necessary for energetic reasons. The high efficiency of these rearrangements suggest that unstable carbonium ions never form even when energetically accessible, rather rearrangement in the reaction complex occurs. Vibrational excitation of NO⁺(*v*) has only a small effect on halide transfer, but does drive it in selected reactions, the most evident being the relatively

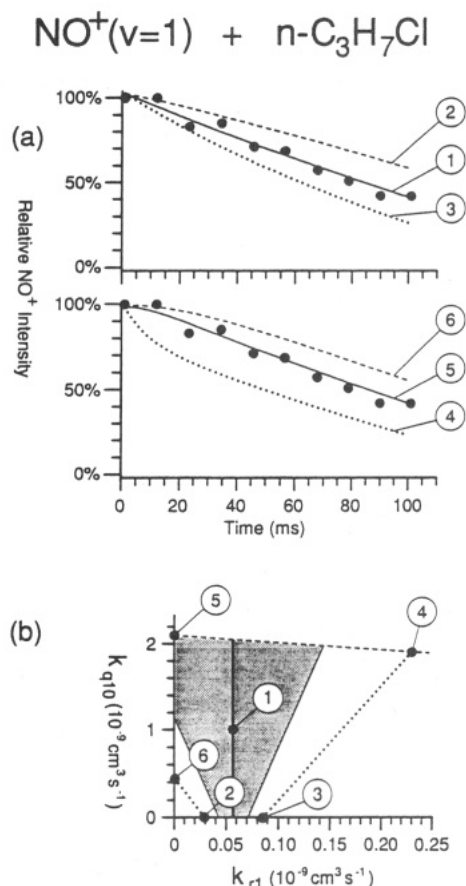
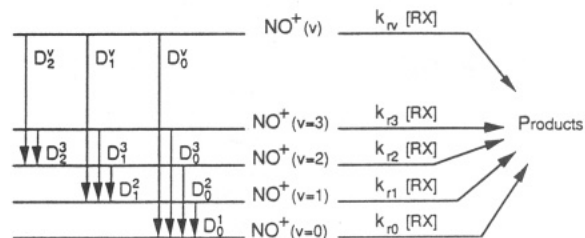
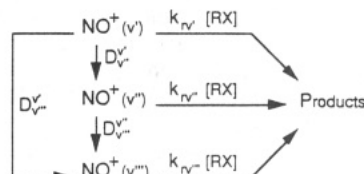


Figure 8. (a) Simulations (lines) along with experimental data (dots) for the NO⁺(*v* = 1) + *n*-C₃H₇Cl system. Parameters used in the simulations 1–6 are shown in the lower diagram (b). Parameter pairs (*k*_{r1}, *k*_{q10}) within the gray zone yield simulations which agree well with the experimental data (e.g., simulation number 1 and 5). *k*_{r0} = 0.057 × 10^{−9} cm³ s^{−1}.

SCHEME IV



SCHEME V



slow reaction NO⁺(*v*) + *n*-C₃H₇Cl.

The third reaction channel, C₃H₆NO⁺ formation, is only observed with *n*-propyl and isopropyl chloride where it is dominant for NO⁺(*v* = 0). Increasing vibrational excitation of NO⁺(*v*) inhibits C₃H₆NO⁺ formation and reactivity becomes dominated by chloride transfer for NO⁺(*v* ≥ 2).

Finally, quenching of vibrationally excited NO⁺(*v*) is an important and efficient process in collisions with alkyl halides. There is some evidence that highly excited NO⁺(*v*) might be quenched by more than one vibrational quantum per collision, but further investigations are necessary to clarify this point.

Acknowledgment. The support of The National Science Foundation under Grant CHE-9119752 is gratefully acknowl-

edged. We also wish to thank Dr. P. R. Kemper for helpful discussions regarding instrumental improvements.

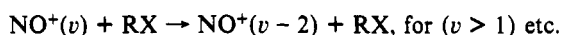
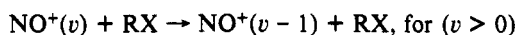
Appendix A

Data Analysis. To analyze the experimental data the following reaction scheme has to be considered:

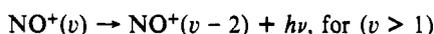
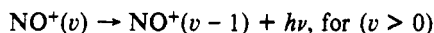
Reaction:



Collisional quenching:



Radiative relaxation:



The same processes are possible for sequential reaction of the product nitric oxide ions $\text{NO}^+(v-1)$, $\text{NO}^+(v-2)$,... as shown in Scheme IV. The different k_{r0} , k_{r1} ,... k_{rv} denote the reaction rate constants, and $[\text{RX}]$ is the halide concentration. The vibrational deactivation from v' to v'' , $D_{v''}^{v'}$, is defined as

$$D_{v''}^{v'} = A_{v''}^{v'} + k_{qv''v'}[\text{RX}]$$

where $A_{v''}^{v'}$ is the Einstein coefficient for spontaneous emission, and $k_{qv''v'}$ is the rate constant for collisional quenching. The Einstein coefficients $A_{v''}^{v'}$ are known from both theory³⁴ and radiative lifetime measurements^{9,11-13} for $v' \leq 5$

$$A_{v''}^{v'} \approx 0 \quad \text{if } v'' < v' - 1$$

$$A_{v''}^{v'} \approx 1/\tau_{v''} \quad \text{if } v'' = v' - 1$$

where $\tau_{v''}$ is the radiative lifetime of $\text{NO}^+(v'')$. The following values for radiative lifetimes are used in the data analysis: $\tau_1 = 90$, $\tau_2 = 45$, $\tau_3 = 31$, $\tau_4 = 24$, and $\tau_5 = 20$ ms.¹³

The differential equations corresponding to Scheme IV can analytically be solved yielding $[\text{NO}^+(v)]$ as a function of time. The unknown parameters k_{r0} , k_{r1} ,... k_{rv} , k_{q10} , k_{q20} ,... k_{qv0} , k_{q21} , k_{q31} ,... k_{qv1} ,... $k_{q,v,v-1}$ can be determined by a least squares fit to the experimental data. To reduce the number of parameters which are determined in the fit and also to reduce the complexity of the problem, the solutions of Scheme V involving only three levels of $\text{NO}^+(v)$ are actually used to fit the data. It turned out that the three level model of Scheme V was sufficient to describe the systems discussed here. It also should be noted that Scheme V is complete when $\text{NO}^+(v)$ is formed in a vibrational state $v \leq 2$. In general, k_{r0} is easily determined by forming NO^+ by REMPI in its vibrational ground state. To evaluate k_{r1} and k_{q10} state-selected $\text{NO}^+(v=1)$ is formed, and the previously determined k_{r0} is kept constant in the fit. Data from higher vibrational levels are similarly analyzed fitting at most two parameters simultaneously, one k_{rv} and if necessary also one $k_{qv''v'}$. In the fitting program used, data collected at different alkyl halide pressures can be included in the same fit. Thus, one fit typically includes between 50 and 100 data points.

If more than one ionic product is formed in Scheme IV, a branching ratio can be determined. If NO^+ is initially formed in the $v=0$ state, the branching ratio $x_{v=0}^{(i)}$ for some channel (i) is given by the ratio of the (i) product ion signal to the sum of all product ion signals ($\sum_i x_{v=0}^{(i)} = 1$). When $\text{NO}^+(v=1)$ is formed by REMPI the observed branching ratio is a convolution of the $v=1$ and the $v=0$ branching ratio (see Scheme IV). Knowing the latter and knowing the equations describing Scheme IV allows us to calculate the $v=1$ branching ratio and by analogy any other $v > 0$ branching ratio.

Appendix B

Error Analysis. The purity of the $\text{NO}^+(v)$ vibrational state formed by REMPI is usually high enough to be of no importance

in the error discussion.^{11,16,17} In some special cases, though, it is a major source of error. The principal impurity in $\text{NO}^+(v)$ is $\text{NO}^+(v+1)$. Hence, the determination of a small rate constant k_{rv} can be quite inaccurate when $k_{r,v+1}$ is very big. However, in all other cases the following sources of error dominate.

Since the total ion signal is not a constant as a function of ion storage time,³⁵ the signal of one ion has to be normalized by the sum of all signals. To do this properly, mass discrimination has to be correctly accounted for. Mass discrimination also has to be corrected for when determining branching ratios. In this work two circumstances make mass discrimination a potentially severe problem. First, experiments have to be performed at relatively high pressure (10^{-6} Torr) in order to make reactions of $\text{NO}^+(v > 0)$ competitive with radiative decay. Therefore, dephasing of the ion packet by collisions after excitation and during signal acquisition is not negligible. Studies carried out in our laboratory show that lighter ions undergoing collisions are dephased much easier than heavy ions, yielding discrimination of the low mass ion signal. By using a short chirp (< 1 ms) and a short acquisition time (2 ms) this effect can be minimized.

Second, in our experiments ion excitation has to be carried out over a large mass (or frequency) range ($m/z = 30$ to 170) making frequency dependent attenuations important. For example, the detection electronics described in ref 15 and used in this work discriminates high frequencies (corresponding to low masses). The amplitude of high frequencies is also attenuated by capacitive loss to ground in coaxial cables and in the ICR cell itself.

In order to get a quantitative description of these mass discrimination effects, experiments with mixtures of Ne, CO, Ar, Kr, and Xe have been carried out. Because the cross sections for electron impact ionization of these gases are well-known, mass discrimination can be determined from the ratio of signal intensities for a known gas mixture ratio. The reproducibility of this method under identical experimental conditions is within $\pm 10\%$.

Pressure has been measured by an ionization gauge calibrated against an MKS Baratron capacitance manometer. While the error of relative pressures is reduced to 1 or 2% with this method, the uncertainty in the absolute pressure might be somewhat higher as calibration reactions (Table VII) indicate.

The same reactions (Table VII) have also been used to study the influence of experimental parameters on rate constants determined. Since the FT-ICR method does not employ a straightforward ion counting type of detection but a rather complex process of ion excitation and Fourier analysis of an induced current, it is not a priori clear how the signal obtained correlates to the ion density in the cell. Even though the total ion density has been kept as low as possible and constant throughout all experiments presented in this work, our studies show that rate constants determined at different instrumental tunings may differ outside the statistical error. Even the ratio of two rate constants may differ somewhat. When all uncertainties are taken into account, we arrive at a conservative error for absolute rate constants of about ($\pm 50\%$). Nevertheless, the results are accurate enough to determine the magnitude of rates and to observe trends as a function of different interesting parameters.

The error in branching ratios, which is determined by the uncertainty of mass discrimination and the statistical error, is about ± 0.1 for values around 0.5 and ± 0.01 for values < 0.05 and > 0.95 .

Appendix C

Quenching. The reactions of $\text{NO}^+(v=0, 1, 2)$ with $\text{C}_3\text{H}_7\text{Cl}$ are analyzed using a model based on Scheme V. The rate constant k_{r0} is readily determined from the $v=0$ data. The $[\text{NO}^+]$ decay curve for $\text{NO}^+(v=1)$ depends on k_{r1} and, if $k_{r1} \neq k_{r0}$, also on k_{q10} . (If $k_{r1} = k_{r0}$, NO^+ disappears equally fast from either level $v=0$ or $v=1$ and thus quenching cannot be seen.) The case $k_{r1} \gg k_{r0}$ has extensively been discussed earlier in the paper for methyl and ethyl iodide where k_{q10} has a significant influence on the shape of the curve. The isopropyl chloride system also belongs in this category (see Figure 7). If on the other hand the experimental $v=1$ decay curve looks about the same as for $v=0$, which is the case for $\text{NO}^+(v=1) + n\text{-C}_3\text{H}_7\text{Cl}$, the question is whether

it is correct to conclude that $k_{r1} \approx k_{r0}$. Simulations compared to experimental data are shown in Figure 8 to clarify this point. It can be seen that k_{r1} values in the range from $0-1.3 \times 10^{-10} \text{ cm}^3 \text{ s}^{-1}$ ($k_{r0} = 0.57 \times 10^{-10} \text{ cm}^3 \text{ s}^{-1}$) yield a very similar curve depending on the value of k_{q10} . The bad determination of k_{r1} also is due to the relatively small value of k_{r0} . If k_{r0} is larger, as is the case for the C₃H₇Br and C₃H₇I systems, k_{r1} is much better determined. While the analysis of the [NO⁺] decay curve in the NO⁺($v = 1$) + n -C₃H₇Cl system yields only an upper limit of $k_{r1} < 1.3 \times 10^{-10} \text{ cm}^3 \text{ s}^{-1}$, we can conclude that $k_{r1} > 0$ since the observed branching ratios are different for the $v = 0$ and $v = 1$ experiments (Figure 2). Quantitative analysis yields $k_{r1} > 0.3 \times 10^{-10} \text{ cm}^3 \text{ s}^{-1}$ which determines k_{r1} within a factor of 5. Similar results hold for determination of k_{rv} for NO⁺($v > 1$) + n -C₃H₇Cl.

Data obtained for NO⁺($v > 2$) are analyzed using a model based on Scheme V ($v'' = v' - 1$, $v''' = v' - 2$). The final results in Table II are the best Scheme V fits in all cases, neglecting NO⁺(v) quenching in the case of n -propyl chloride.

References and Notes

- (1) (a) A brief review of the work prior to 1985 is given: Bowers, M. T. *Advanced Mass Spectrometry*; Todd, J. F. J., Ed.; John Wiley and Sons: New York, 1986; pp 533-551. (b) For more recent and more selective reviews, see: Anderson, S. L. Multiphoton Ionization State Selection: Vibrational Mode and Rotational State Control. *Adv. Chem. Phys.* 1992. Vibrational Mode Effects in Polyatomic Ion Reactions. In *Fundamentals of Gas Phase Ion Chemistry*; Jennings, K. R., Ed.; Kluwer: Amsterdam, 1991.
- (2) See: chapter by Baer, T. In *Gas Phase Ion-Chemistry*; Bowers, M. T., Ed.; Academic Press: New York, 1979; Vol. 1.
- (3) See, for example: Böhringer, H.; Durup-Ferguson, M.; Fahey, D. W.; Fehsenfeld, F. C.; Ferguson, E. E. *J. Chem. Phys.* 1983, 79, 4201.
- (4) Kemper, P. R.; Bowers, M. T.; Parent, D. C.; Mauclaire, G.; Derai, R.; Marx, R. *J. Chem. Phys.* 1983, 79, 160.
- (5) Conway, W. E.; Morrison, R. J.; Zare, R. N. *Chem. Phys. Lett.* 1985, 113, 429.
- (6) (a) See, for example: Conway, W. E.; Ebata, T.; Zare, R. N. *J. Chem. Phys.* 1987, 87, 3453. (b) See, for example: Orlando, T. M.; Yang, B.; Chiu, Y.; Anderson, S. L. *J. Chem. Phys.* 1990, 92, 7356.
- (7) Dobler, W.; Federer, W.; Howorka, F.; Lindinger, W.; Durup-Ferguson, M.; Ferguson, E. E. *J. Chem. Phys.* 1983, 79, 1543.
- (8) Federer, W.; Dobler, W.; Howorka, F.; Lindinger, W.; Durup-Ferguson, M.; Ferguson, E. E. *J. Chem. Phys.* 1985, 83, 1032.
- (9) Heninger, M.; Fenistein, S.; Durup-Ferguson, M.; Ferguson, E. E.; Marx, R.; Mauclaire, G. *Chem. Phys. Lett.* 1986, 131, 439.
- (10) Morris, R. A.; Viggiano, A. A.; Dale, F.; Paulson, J. F. *J. Chem. Phys.* 1988, 88, 4772.
- (11) Kuo, C.-H.; Beggs, C. G.; Kemper, P. R.; Bowers, M. T.; Leahy, D. J.; Zare, R. N. *Chem. Phys. Lett.* 1989, 163, 291.
- (12) Fenistein, S.; Heninger, M.; Marx, R.; Mauclaire, G.; Yang, Y. M. *Chem. Phys. Lett.* 1990, 172, 89.
- (13) Wyttenbach, T.; Beggs, C. G.; Bowers, M. T. *Chem. Phys. Lett.* 1991, 177, 239.
- (14) Williamson, A. D.; Beauchamp, J. L. *J. Am. Chem. Soc.* 1975, 97, 5714.
- (15) (a) The word "statistical" is used here in a restricted sense: detailed state counting and angular momentum are not considered. Rather, the presumption is that all collisions with enough energy to react (in the Boltzman sense) do so with a Boltzman probability. (b) Beggs, C. G.; Kuo, C.-H.; Wyttenbach, T.; Kemper, P. R.; Bowers, M. T. *Int. J. Mass Spectrom. Ion Proc.* 1990, 100, 397.
- (16) Miller, J. C.; Compton, R. N. *J. Chem. Phys.* 1981, 75, 22.
- (17) Ebata, T.; Zare, R. N. *Chem. Phys. Lett.* 1986, 130, 467.
- (18) Su, T.; Bowers, M. T. In *Gas Phase Ion Chemistry*; Bowers, M. T., Ed.; Academic: New York, 1979; Vol. 1, pp 83-118.
- (19) Lias, S. G.; Bartmess, J. E.; Liebman, J. F.; Holmes, J. L.; Levin, R. D.; Mallard, W. G. *Gas-Phase Ion and Neutral Thermochemistry, Journal of Physical and Chemical Reference Data*; 1988; Vol. 17, Suppl. 1.
- (20) Ferguson, E. E. *J. Phys. Chem.* 1986, 90, 731.
- (21) Moore, C. B. *J. Chem. Phys.* 1965, 43, 2979.
- (22) Beswick, J. A.; Jortner, J. *J. Chem. Phys.* 1978, 68, 2277.
- (23) Johnson, K. E.; Wharton, L.; Levy, D. H. *J. Chem. Phys.* 1978, 69, 2719.
- (24) Laudenslager, J. B.; Huntress, W. T., Jr.; Bowers, M. T. *J. Chem. Phys.* 1974, 61, 4600.
- (25) Houle, F. A.; Anderson, S. L.; Gerlich, D.; Turner, T.; Lee, Y. T. *J. Chem. Phys.* 1982, 77, 748.
- (26) Kimura, K.; Katsumata, S.; Achiba, Y.; Yamazaki, T.; Iwata, S. *Handbook of Hel Photoelectron Spectra of Fundamental Organic Molecules*; Japan Scientific Soc.: Tokyo, 1981.
- (27) Huber, K. P.; Herzberg, G. *Constants of Diatomic Molecules*; Van Nostrand Reinhold: New York, 1979.
- (28) Durup-Ferguson, M.; Böhringer, H.; Fahey, D. W.; Ferguson, E. E. *J. Chem. Phys.* 1983, 79, 265.
- (29) Alge, E.; Lindinger, W. *J. Geophys. Res.* 1981, 86, 871.
- (30) Yang, B.; Chiu, Y.-H.; Anderson, S. L. *J. Chem. Phys.* 1991, 94, 6459.
- (31) Rosenstock, H. M.; Buff, R.; Ferreira, M. A. A.; Lias, S. G.; Parr, A. C.; Stockbauer, R. L.; Holmes, J. L. *J. Am. Chem. Soc.* 1982, 104, 2337.
- (32) Brand, W. A.; Baer, T.; Klots, C. E. *Chem. Phys.* 1983, 76, 111.
- (33) Traeger, J. C. *Int. J. Mass Spectrom. Ion Phys.* 1980, 32, 309.
- (34) Werner, H.-J.; Rosmus, P. *J. Mol. Spectrosc.* 1982, 96, 362. Chambaud, G.; Rosmus, P. *Chem. Phys. Lett.* 1990, 165, 429. Partridge, H.; Langhoff, S. R.; Bauschlicher, C. W., Jr. *Chem. Phys. Lett.* 1990, 170, 13.
- (35) Moini, M.; Eyler, J. R. *Int. J. Mass Spectrom. Ion Proc.* 1989, 87, 29.
- (36) Dyke, J.; Ellis, A.; Jonathan, N.; Morris, A. J. *Chem. Soc., Faraday Trans. 2* 1985, 81, 1573.
- (37) Raghavachari, K.; Whiteside, R. A.; Pople, J. A.; Schleyer, P. v. R. *J. Am. Chem. Soc.* 1981, 103, 5649.
- (38) Ikezoe, Y.; Matsuoaka, S.; Takebe, M.; Viggiano, A. *Gas Phase Ion Molecule Reaction Rate Constants through 1986*; Maruzen: Tokyo, 1987.
- (39) Anicich, V. G.; Blake, G. A.; Kim, J. K.; McEwan, M. J.; Huntress, W. T., Jr. *J. Phys. Chem.* 1984, 88, 4608.
- (40) See ref 24.
- (41) Kemper, P. R.; Bowers, M. T. *Int. J. Mass Spectrom. Ion Phys.* 1983, 52, 1.
- (42) Marx, R.; Mauclaire, G.; Derai, R. *Int. J. Mass Spectrom. Ion Phys.* 1983, 47, 155.
- (43) Jaffe, S.; Klein, F. S. *Int. J. Mass Spectrom. Ion Phys.* 1974, 14, 459.
- (44) Huntress, W. T., Jr.; McEwan, M. J.; Karpas, Z.; Anicich, V. G. *Astrophys. J. Supp. Ser.* 1980, 44, 481.
- (45) See ref 44.
- (46) Myher, J. J.; Harrison, A. G. *J. Phys. Chem.* 1968, 72, 1905.
- (47) Harrison, A. G.; Myher, J. J.; Thynne, J. C. *J. Adv. Chem. Ser. No.* 1966, 58, 150.
- (48) Lifshitz, C.; Gleitman, Y.; Gefen, S.; Shainok, U.; Dotan, I. *Int. J. Mass Spectrom. Ion Phys.* 1981, 40, 1.
- (49) Fehsenfeld, F. C.; Ferguson, E. E.; Schmeltekopf, A. L. *J. Chem. Phys.* 1966, 45, 404.
- (50) Rakshit, A. B.; Warneck, P. *J. Chem. Phys.* 1980, 73, 2673.
- (51) Thomas, R.; Barassin, A.; Burke, R. R. *Int. J. Mass Spectrom. Ion Phys.* 1978, 28, 275.
- (52) Dotan, I.; Lindinger, W. *J. Chem. Phys.* 1982, 76, 4972.
- (53) Rakshit, A. B.; Stock, H. M. P.; Wareing, D. P.; Twiddy, N. D. *J. Phys. B* 1978, 11, 4237.
- (54) Shul, R. J.; Upschulte, B. L.; Passarella, R.; Keesee, R. G.; Castleman, A. W., Jr. *J. Phys. Chem.* 1987, 91, 2556.
- (55) Sieck, L. W.; Gordon, R., Jr. *J. Res. Nat. Bur. Stand.* 1974, 78A, 315.
- (56) Adams, N. G.; Smith, D.; Grief, D. *Int. J. Mass Spectrom. Ion Phys.* 1978, 26, 405.
- (57) Fehsenfeld, F. C.; Schmeltekopf, A. L.; Ferguson, E. E. *J. Chem. Phys.* 1966, 45, 23.
- (58) Smith, D.; Adams, N. G.; Miller, T. M. *J. Chem. Phys.* 1978, 69, 308.
- (59) Fehsenfeld, F. C.; Schmeltekopf, A. L.; Ferguson, E. E. *J. Chem. Phys.* 1966, 44, 4537.
- (60) Tichý, M.; Rakshit, A. B.; Lister, D. G.; Twiddy, N. D.; Adams, N. G.; Smith, D. *Int. J. Mass Spectrom. Ion Phys.* 1979, 29, 231.